Accepted Manuscript
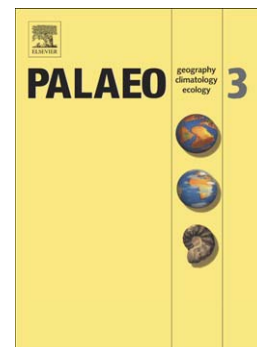
High resolution δ^{18}O seasonality record in a French Eemian tufa stromatolite (Caours, Somme Basin)

J. Dabkowski, S.H. Royle, P. Antoine, A. Marca-Bell, J.E. Andrews

Please cite this article as: Dabkowski, J., Royle, S.H., Antoine, P., Marca-Bell, A., Andrews, J.E., High resolution δ^{18}O seasonality record in a French Eemian tufa stromatolite (Caours, Somme Basin), *Palaeogeography, Palaeoclimatology, Palaeoecology* (2015), doi: 10.1016/j.palaeo.2015.08.017

High resolution δ^{18}O seasonality record in a French Eemian tufa stromatolite (Caours, Somme Basin)

J. Dabkowski[a,b,][*][1], S. H. Royle[c], P. Antoine[a], A. Marca-Bell[c] and J. E. Andrews[c]

[a]Laboratoire de Géographie Physique (UMR-CNRS 8591), 1 place Aristide Briand, 92195 Meudon cedex, France

[b]Département de Préhistoire du Muséum National d'Histoire Naturelle (UMR 7194), 1, rue René Panhard, 75013 Paris, France

[c]School of Environmental Sciences, University of East Anglia, Norwich, NR4 7TJ, United Kingdom

*Corresponding author. Tel. +336 89 72 25 03.

E-mail address: julie.dabkowski@geoarcheon.fr

Abstract

Recent and sub-recent laminated tufa stromatolites can contain high resolution δ^{18}O records of in stream temperature change. Fossil tufa stromatolites are therefore key targets for reconstructing terrestrial palaeoclimatic, but so far only a few examples have been published. In this research we studied a 2.5 cm-radius tufa stromatolite from the Eemian of the Somme Basin, Northern France. We show; (1) that high resolution sampling of fossil laminated tufas is highly reproducible. We demonstrate; (2) that within the limitations of the δ^{18}O method, NW European Eemian seasonality was essentially similar to the present day. Perhaps most important we show; (3) that precise observations from thin section that match the position of

[1] Present address: GéoArchÉon, 30 rue de la Victoire, 55210 Viéville-sous-les-Côtes, France

lamina boundaries with the position of reversals in direction of $\delta^{18}O$ values, are a record of the style or intensity of seasonality. In this French tufa stromatolite abrupt $\delta^{18}O$ reversals do not coincide with sharp lamina boundaries; rather the lamina boundaries occur where $\delta^{18}O$ values are either gradually decreasing or increasing. We interpret this to be a record of abrupt changes in the growth rate, accelerating in spring or early summer and decelerating in late autumn or early winter. This contrasts with a published montane record from the Eemian of Greece, where lamina boundaries and $\delta^{18}O$ reversals do coincide, interpreted as more extreme seasonality caused by cessations in growth due to summer aridity or winter cold. We thus propose this criterion as a method to help identify regional styles of seasonality in tufa stromatolites.

1. Introduction

The advent of micromilling technologies combined with increased sensitivity of gas source mass spectrometers has enabled ever higher resolution sampling and analysis of materials that contain seasonal palaeoclimate information such as coral skeletons and speleothems. Laminated tufa deposits, the subject of this paper, have also shown much promise as seasonal palaeoclimatic proxies through their stable isotope records in both temperate (e.g. Matsuoka et al. 2001) and wider climatic settings (e.g. Ihlenfeld et al., 2003; Kano et al. 2007). Early papers concentrated on environmentally well-characterised recent and sub-recent deposits (Matsuoka et al. 2001; Kano et al., 2003) that established the potential for recovery of seasonal palaeoclimatic records. In the early 2000s particular scrutiny was also given to the timing and micromorphology of the seasonal laminae, with Kano et al. (2003) proposing that the principal control on lamination is the calcite precipitation rate (Kwai et al., 2009), albeit modulated by availability of seasonal rainfall, particularly in the sub tropics (Liu et al., 2010). This was followed by a number of case studies from ancient tufa stromatolites (O'Brien et al., 2006; Mischke and Zhang 2008) that demonstrated the validity of the approach and extended some of the criteria for successful interpretation. In particular, Brasier et al. (2010; 2011) drew attention to the nature of sharp lamina boundaries in montane Mediterranean tufas and inferred these represented breaks in tufa precipitation.

In this paper we emphasise two areas that contribute to the interpretation of high resolution stable isotope records in tufa stromatolites. First we present replicate isotopic data transects that demonstrate for the first time the reproducibility of the approach in fossil tufas. Second we investigate the relationship between sharp lamina boundaries and the isotopic transect, emphasising that the timing of isotopic 'reversals' between higher and lower values are critical in correctly interpreting the palaeoclimatic signal.

This study is based on tufa stromatolites from a Last Interglacial deposit at Caours (Northern France; 50°07'N, 01°52'E; Fig. 1A) where the overall palaeoclimatic context is already established (Dabkowski et al., 2011). This presents an opportunity to decipher some details of N. European seasonal paleoclimate signals in an interglacial period that many take as a possible model for a near future 'anthropogenically warmed' climate (Van Kolfschoten et al., 2003; McManus et al., 2003; Sánchez-Goñi, 2007).

The tufa overlies lower terrace fluvial deposits of the Scardon, a tributary of the river Somme; its area is >10 000 m^2 and it is up to 3.5 m thick. Archaeological excavations (dir. J.L. Locht, INRAP Picardie) of a Middle Palaeolithic site at the base of the tufa have provided excellent stratigraphic profiles that show the tufa overlying periglacial alluvial sediments corresponding to the penultimate stage of infilling valley gravels attributed to MIS 6 in the Somme basin (Antoine et al., 2006). Dating is based on 12 U/Th and ESR/U-Th dates, which yield an Eemian age of 122 ± 8 ka (Antoine et al., 2006; Bahain et al., 2010). Bioclimatic data from molluscs, ostracods and leaf imprints support the age assignation recording a transition from a cold stage (interpreted as Saalian) into a warmer stage (interpreted as Eemian; MIS 5e), with a climatic optimum identified by mollusc assemblages in a thin organic tufa horizon in the lower part of the sequence. The tufa is truncated and overlain by Weichselian Early-glacial humic soils corresponding to MIS 5d to 5a (Antoine et al., 2006).

Well calcified deposits, including tubular tufa-stromatolites with concentric lamination, are locally abundant and very-well preserved within the tufa sequence (Antoine et al., 2006). These detritus-free tufa stromatolites preserve clear lamination making them excellent targets for high resolution petrographic and isotopic investigation of seasonally distinct climatic and

4

environmental conditions (Chafetz and Folk, 1984; Freytet and Plet, 1991; Freytet and Verrecchia, 1998; Kano et al., 2003; Andrews and Brasier, 2005).

For this study we selected a well-preserved, crystalline stromatolite from Caours sector S2 (excavated in 2005). Here the tufa is mainly a massive crumbly white to light grey deposit with very low detrital content. These tufa units are laterally extensive (tens m²) and prograde parallel to slope, a configuration characteristic of spring-line tufa formations (Casanova, 1981; Weisrock, 1981; Pedley, 1990). The tufa is built by the cyanobacterial morphotaxon *Broutinella sp.* (Freytet, 1998) associated with aquatic molluscs and ostracodes (Dabkowski et al., 2010) that indicate permanent shallow water flowing downslope from springs.

Small channels (0.5 to 1 m width) cut through the more extensive massive tufa units, and are interpreted as co-genetic with the main deposition phase (Fig. 1B and C). The channels contain oncoid-rich facies, indicative of shallow running water, routing flow from feeder spings downslope to the palaeo-Scardon valley (Antoine et al., 2006). The studied stromatolite was sampled at the top of one of these small channels. These stromatolites formed by encrustation around plant stems (1-2 mm in diameter) constructing a tubular mass ~2.5 cm-radius and 40-50 cm-high. In hand specimen, polished cross-sections show alternation of clear translucent and darker porous laminae (Fig. 2).

2. Materials and methods

Petrography was done using one large non-impregnated thin section of the whole cross-section of the stromatolite to identify cyanobacterial/algal taxa, establish microfacies and the nature and position of microfacies boundaries, and to identify diagenetic fabrics.

Samples for $\delta^{18}O$ and $\delta^{13}C$ were drilled from three transects using a Micromill (Fig. 2). Three separate transects covering the same growth interval were made to allow assessment of the reproducibility of the isotopic records. Samples were drilled parallel to growth direction of the stromatolite and the spacing between samples was approximately 200 μm with the mill set to take sample trenches 20 μm wide and 100 μm deep.

The first transect was split into two 6 mm wide sections avoiding an area of indistinct laminae and porous tufa between them (Str-HR, 33 samples and Str-HR2, 36 samples; Fig. 2). This transect was re-drilled from exactly the same position after the slab face had been re-polished. This second transect was about 24 mm long (Str-HRc, 70 samples; Fig. 2) and included the porous, indistinct area previously avoided. Finally, a replicate transect (Str-HRr, 78 samples) was drilled to the left of the two others. The sampling area here was slightly curved with more irregular laminae than the first location. The Micromill was thus programmed to follow each laminae as closely as possible, minimising any 'smoothing' of the signal at lamina boundaries that might otherwise result from mixing material from different laminae.

Isotopic analyses were made on CO_2 derived from 100 ±10 μg carbonate material reacted with anhydrous H_3PO_4 at 90°C in a common acid bath automated preparation system online with a Europa SIRA mass spectrometer. Repeated analyses of the laboratory standard (n=64) gave a 2σ precision of less than ±0.1 ‰ for both $\delta^{18}O$ and $\delta^{13}C$.

3. Results

3.1. Petrography

The stromatolite is wholly composed of micritic to sparitic calcite; no detrital grains were seen and evidence of preserved organic matter is sparse. Four microfacies were determined,

labelled I to IV (Fig. 2). Their alternation corresponds to the translucent and darker porous laminae seen in hand specimen.

Microfacies I and II are best represented (Fig. 2), the first corresponding to continuous sparitic laminae with crystal long axes of a few hundred microns to about 3 mm. In some cases, internal laminae are present, underlain by very thin organic horizons (Fig. 2). Microfacies II is of micritic to microsparitic composition, typically a few tens to 200-300 μm thick with continuous wavy to planar internal laminae (Fig. 2). Cyanobacterial/algal filaments are not usually visible in either Microfacies I or II; where they are present, usually in Microfacies I, the filaments are 3-5 μm in diameter more or less erect, well-spaced, parallel to the growth direction, and forming fascicules of various shapes.

Microfacies III corresponds to the very porous laminae seen in hand specimen. Sparitic crystals including filaments and fascicules, similar to those in Microfacies I, form discontinuous, vuggy and disorganised laminae (Fig. 2).

Microfacies IV is a clotted micrite lacking internal lamination or cyanobacterial/algal filament structure (Fig. 2). This microfacies forms a 0.5 cm thick lamina, interrupted by two 10-20 μm thick sparitic layers (dotted lines on Fig. 2); microsparitic crystals are also observed around the edges of vugs. This microsparite is the only clear evidence of neomorphic alteration and the mass of calcite of this type is small. No other clearly diagnostic diagenetic fabrics were observed.

The boundaries between laminae formed by these different microfacies are sharp (Fig. 2) and drawn precisely on Figure 3.

3.2.   Stable isotopes

The stable isotope data are summarised in Table 1 and the data sets are available as Supplementary Material. The three transects show equivalent data sets with similar ranges, means and standard deviation for both carbon and oxygen (Table 1). Oxygen isotope values range between -6.6 and -3.9 ‰ with an identical mean value of -5.2 ‰ for each transect; $\delta^{13}C$ values range between -11.2 and -6.8 ‰ with the same -10.0 ‰ mean value for each transect (Table 1). The ranges and means of the tufa stromatolite are essentially the same as those for the deposit as a whole (mean $\delta^{18}O$ -5.4 and mean $\delta^{13}C$ -10.1‰; Dabkowski et al., 2011) such that the tufa stromatolite should be a representative 'spot sample' from the deposit. There is statistically significant (Table 1) but weak (26-35% based on r^2) co-variation between $\delta^{18}O$ and $\delta^{13}C$ in each transect and the $\delta^{18}O$ and $\delta^{13}C$ ranges are consistent with maritime temperate tufa data from NW Europe where aridity and evaporation effects are low (Andrews, 2006).

Each data transect is plotted in Figure 3: the three transects contain slightly different numbers of samples (Table 1) due to natural variability of lamina width, such that sample density in each lamina is slightly different in each transect. For this reason, that data were not grouped 'globally' for statistical correlation. Nevertheless comparison of the three transects and their running means (Fig. 3) leave no doubt about the reproducibility of the data. Variations in $\delta^{18}O$ and $\delta^{13}C$ >0.5‰ are non-random and attributable to either an environmental or diagenetic driver.

The lowest $\delta^{18}O$ values come from sparitic Microfacies I; the other microfacies contain broadly less negative values, but without clear distinctions between them. This microfacies/isotopic relationship is most obvious in the upper part (15-22 mm) of Str-HRr and in the corresponding part of the other transects. In Str-HR 2 and Str-HRc, the two thin microsparitic horizons in Microfacies IV (dotted lines on Fig. 2 and 3 between 2 and 5 mm) are also associated with lower $\delta^{18}O$ values.

In all transects, the δ^{13}C profiles are fairly smooth but with an overall shape broadly similar to δ^{18}O. δ^{13}C values are least negative in the basal 6 mm, starting around -7‰, becoming broadly more negative until stabilizing at values around -10.5‰ at 6 mm.

4. Interpretation and discussion

4.1. Seasonal control of lamina microfacies

The arrangement of cyanobacterial/algal filaments and fascicules in Microfacies I-III, is diagnostic of the morphotaxa *Broutinella arvenensis* (Freytet, 1998). In the holotype, Freytet (1998) describes variably micritic to sparitic fabrics including continuous wavy to planar internal laminations, often underlain by thin organic horizons, which is very similar to the material described here, particularly Microfacies I. While this morphotaxon has no biological significance (Freytet 1997) *B. arvenensis* is thought to represent the modern cyanobacterial genera *Phormidium* and *Schizothrix* (Freytet, 1998). These are known to constitute an algal biocenose where one is predominant during spring and the other during autumn, generating alternating laminae (Freytet, 1992; Freytet and Plet, 1996). It is thus inferred that the tufa stromatolite laminae formed under seasonal conditions. Microfacies IV has no clear cyanobacterial/algal structure: it is interpreted here as a microbial fabric but is not assigned to specific taxa.

A clear feature of the microfacies pattern (Fig. 2) is the rhythmic presence of sparitic Microfacies I. While a few authors consider such fabrics diagenetic (Janssen et al., 1999; Janssen, 2000), others interpret them as primary (see review in Andrews and Brasier, 2006). In Microfacies I the preservation of cyanobacterial filaments argue against a diagenetic origin (Brasier et al., 2011), the presence of expanded fascicules suggesting growth conditions favourable for cyanobacterial colonies. In laminated European tufas, alternation of dense micritic laminae and more porous laminae containing erect cyanobacterial/algal filaments

have typically been shown to correspond to autumn/winter and spring/summer conditions respectively (Freytet, 1990; Freytet and Plet, 1996; Janssen et al., 1999), possibly resulting from the 'autumn-winter bias' of meteoric recharge (Kano et al. 2003).

We interpret Microfacies I calcite crystals to have grown in spring-summer under strong solar illumination and warm temperatures; these 'summer' laminae correspond to the lowest $\delta^{18}O$ values, and to some of the lowest $\delta^{13}C$ values, although the latter relationship is not marked. The other microfacies are interpreted to represent more limited cyanobacterial and microbial growth under cooler conditions, corresponding with less negative $\delta^{18}O$ values.

In our sample transects, six clear Microfacies I laminae represent spring-summer conditions (shown in red, Fig. 2 and 3) not including two continuous sparitic layers that interrupt Microfacies IV (shown by pecked lines in Fig. 2 and 3). These alternate with five clear layers corresponding to winter conditions (shown in blue, Fig. 2 and 3). On this basis six annual cycles are covered by the sampling transects. We find no evidence of pervasive diagenetic alteration, except, possibly, the small amounts of microspar around vug margins in Microfacies IV; thus we infer that the tufa geochemistry is a record of seasonal changes preserved at the time of deposition.

 The boundaries between these seasonal layers are quite distinct, but not marked by increased presence of clay or organic detritus. In the absence of physical evidence it is difficult to be diagnostic about the cause of these sharp boundaries. However, it is also clear that reversals in $\delta^{18}O$ values typically <u>do not</u> coincide with these lamina boundaries. We discuss the significance of this observation in section 5 below.

4.2. Stable isotopes

4.2.1. Stable oxygen isotopes

The depositional microfacies indicate tufa formation in shallow channels with more or less continuously flowing water, with low evaporation effects as confirmed by the weak co-variation between $\delta^{18}O$ and $\delta^{13}C$.

Most in-stream shallow water tufas deposit calcite in near isotopic equilibrium with depositing waters a few hundred metres downstream of the spring resurgence (Matsuoka et al. 201; Andrews 2006; Sun et al., 2014). In fossil settings it is more difficult to infer the physical relationship between source springs and deposit: however, comparative sedimentology and robust microfacies interpretations are the basis for inferring that palaeo-calcites, from stream-sited tufas, formed in near isotopic equilibrium. Under near-equilibrium conditions, variations in tufa $\delta^{18}O$ are caused mainly by; (1) variation in the isotopic composition of the water from which tufa calcite precipitates and/or, (2) change in the water temperature of the stream at the time of calcite precipitation.

Change in the isotopic composition of the tufa precipitating water is caused by changes in the mean annual isotopic composition of the meteoric water that recharges groundwater-fed springs (Clark and Fritz, 1997; Darling, 2004). The local bedrock at Caours is Upper Turonian Chalk, the main aquifer on the northern edge of the Paris Basin. Chalk aquifers have groundwater residence characteristics that typically result in seasonally smoothed groundwater isotopic compositions (Darling et al., 2003) although in some cases seasonal signals can be transmitted if the unsaturated zone is <5 m thick, or if local flow paths to a spring are short (Darling et al., 2003). We cannot be sure exactly what the Eemian recharge characteristics were for this Chalk aquifer but we can make a comparison with the modern system as a starting point, making the assumption that the difference between modern and Eemian climatic systems would not have been large (Sánchez-Goñi, 2007; van Kolfschoten et al., 2003). Today, this part of continental NW Europe has a temperate oceanic climate with annual precipitation around 650-750 mm, distributed quite uniformly through the year, with

11

slightly higher precipitation amount in Oct-Nov-Dec (Table 2). Monthly mean $\delta^{18}O$ of modern precipitation is recorded at GNIP (Global Network of Isotopes in Precipitations; IAEA/WMO, 2006), stations, the closest to Caours being Liège (Belgium), Brest and Orléans (France). At these stations maximum $\delta^{18}O$ is recorded during the summer months (June or July), while minima occur in winter (in December or January; Table 3). If seasonal changes in the isotopic composition of groundwater-fed spring water were transmitted, then the lowest values should reflect the isotopically light composition of autumn and early winter rainfall recharge. This is the converse of our microfacies interpretation, where the lowest $\delta^{18}O$ values correspond with 'spring-summer' laminae. Moreover, we are sceptical that these seasonal isotopic recharge characteristics would have survived homogenisation in the Chalk aquifer before resurgence at the feeding springs.

Given the above, we think it unlikely that seasonal variation in water isotopic composition contributed much to the observed isotopic variation in the tufa record. We are more persuaded that the sub-annual to annual sampling resolution achieved in this study is largely a record of in-stream changing water temperature, with increasing $\delta^{18}O$ in tufa calcite caused by decreasing water temperature (Matsuoka et al., 2001; Andrews, 2006; O'Brien et al., 2006; Hori et al., 2009) and vice versa. The lowest $\delta^{18}O$ values, on this basis the warmest water temperatures, are thus associated with the 'spring-summer' laminae of Microfacies I (Fig. 3). The other microfacies correspond to higher $\delta^{18}O$ values which we assigned broadly to cooler conditions (microfacies II, III and IV). Our independent interpretations of petrographical and stable isotope data are strongly coherent and consistent with the majority of NW European tufa systems (reviewed in Andrews and Brasier 2005; Andrews 2006).

As the isotopic composition of the stream water is unknown we cannot use a palaeotemperature equation to calculate precise temperatures, but we can use palaeotemperature formulations to estimate likely values and relative changes in seasonal temperature using water $\delta^{18}O$ values based on modern data. In Table 4 we give estimated temperature ranges based on: (1) mean $\delta^{18}O$ of Holocene groundwater in the nearby Paris Basin (Dray et al. 1998), which should be similar to the mean MIS 5 groundwater value; (2) mean interpolated $\delta^{18}O$ (OIPC; v.2.2, Bowen and Revenaugh 2003) for modern summer recharge (April-October), and (3) mean interpolated $\delta^{18}O$ (OIPC) for modern winter recharge (November-March) at Caours.

There is a growing body of field data (e.g. Sun et al., 2014) that relates tufa calcite deposition rate to known stable isotopic fractionation factors. The relationship of Kim and O'Neil (1997) was found most appropriate for fast depositing tufas by Sun et al. (2014) whereas slower growing tufa calcites were better described by the Coplen (2007) equilibrium relationship, which concurs with the laboratory results of Watkins et al. (2013). While we do not know the growth rate of our tufa, Kwai et al., (2009) noted that annual lamination was best developed in relatively slow growing tufas; this might imply that the Coplen (2007) relationship is best suited to our samples, but we use both relationships, and two other appropriate formulations, to calculate the full range of notional temperatures (Table 4).

The results show that the range in tufa $\delta^{18}O$ (-6.3 and -4.2‰) indicates a seasonal change of stream water temperature of between 8 and 10 ˚C depending on the palaeotemperature equation used. We can compare this with appropriate modern water temperature ranges: (1) in tufa precipitating streams in NW Europe, where the range is ~ 9 ˚C typically between 8-17 ˚C (Andrews et al. 1997; Garnett et al. 2004); (2) for modern springs, Hameau Bouillancourt and

Nouvion, within 15 km of Caours, where the seasonal range is ≤ 10 ˚C between 5-15 ˚C (stations' European codes are FR00328X0014/HY and FR00324X0043/HY respectively; data source: Agence de l'Eau Artois-Picardie – AEAP, in the online French national groundwater database: www.ades.eaufrance.fr); and (3) with the more mature Scardon River at Abbeville (2 km from Caours) where the seasonal range was ~12 ˚C between 1970 and 2010 (station 1410000; data source: AEAP; www.eau-artois-picardie.fr). These comparisons, particularly cases 1 and 2, suggest that the calculated temperature ranges are reasonable. Also, the temperatures calculated using mean $\delta^{18}O$ for modern Caours winter recharge (Tab. 4) are not realistic, with summer temperatures < 9 ˚C and negative winter temperatures. This is a strong indication that winter meteoric recharge with $\delta^{18}O$ around -9‰ was not a dominant component of the spring water and that the groundwater probably had a $\delta^{18}O$ close to -7‰, resulting in summer temperatures around 12-18 ˚C depending on the palaeotemperature equation used.

4.2.2. Stable carbon isotopes

The $\delta^{13}C$ values in the tufa as a whole are typical of those recorded in modern vegetated NW European river valleys (Andrews, 2006); however, the high resolution record is neither simple nor predictable with microfacies changes or with $\delta^{18}O$. On the sub-annual time-scales of interest here, the relative effects of seasonal soil-air contribution (Hori et al. 2008), CO_2 degassing and upstream/in-aquifer calcite precipitation (Ihlenfeld et al., 2003) are probably the most important contributors to the variability in $\delta^{13}C$. In a modern Japanese tufa system Matsuoka et al. (2001) showed strong $\delta^{13}C$ covariation between calcite and dissolved inorganic carbon $\delta^{13}C$ ($\delta^{13}C_{DIC}$). They demonstrated that $\delta^{13}C_{DIC}$ is dependent on degassing/calcite precipitation (prior calcite precipitation - PCP) processes in the aquifer. These effects can be stronger in winter when the atmospheric air temperature is cooler (and so

denser) and thus its contrast with aquifer air temperature is more marked. The induced ventilation decreases the in-aquifer pCO_2 favouring degassing and PCP. Increased PCP in winter implies that $\delta^{13}C_{DIC}$ (and so tufa calcite $\delta^{13}C$) should increase under cooler conditions (Matsuoka et al., 2001). Our Eemian $\delta^{13}C$ data can be interpreted in this way: it helps explain some of the statistical covariation between $\delta^{18}O$ and $\delta^{13}C$ (see also Matsuoka et al., 2001) and is coherent with the independent seasonal interpretation of the petrographic data.

5. Lamina boundaries and $\delta^{18}O$ reversals

An important outcome of this study is the discovery that the $\delta^{18}O$ reversals (Fig. 3) do not coincide with lamina boundaries; rather the lamina boundaries occur where $\delta^{18}O$ values are either gradually decreasing or increasing. This discovery contrasts with earlier work on a MIS 5 laminated *Phormidium* tufa stromatolite in central Greece (Brasier et al., 2010; Fig. 4) where $\delta^{18}O$ showed abrupt reversals coincident with lamina boundaries (Fig. 4). In the Greek montane tufa the sharp lamina/microfacies boundaries were interpreted as temporary cessations of microbial growth caused by extreme dry summers and very cold winter conditions limiting microbial growth to the spring and autumn seasons.

The Caours lamina boundaries do not appear to record 'extreme growth interruptions' caused by desiccation or winter cold. Such cessation of stromatolite growth might be expected to be marked physically by, for example, erosion surfaces and/or detritus accumulating on the growth surface, subsequently encrusted by the next phase of growth. However, in our specimen, the lack of clay or organic detrital layers indicates near-continuous calcite precipitation, the sharp transitions between laminae simply representing abrupt change in the rate of growth (spring to summer and the again autumn to winter), as implied for a Belgian tufa stromatolite by Monty (1976, p. 207-208).

15

These differences in the synchronicty of δ^{18}O reversals and lamina boundaries suggest that tufa stromatolites may record different styles of seasonality, distinguishing in this case Mediterranean montane climates (Greece) that experience 'extreme seasonality' in terms of winter recharge and summer aridity, from more oceanic and less extreme (NW France) seasonal climate where changes in temperature and aridity are more gradual.

6. Conclusions

This study presents two new discoveries that will help in the on-going research into high-resolution palaeoclimatic records in tufa stromatolites.

1. We show for the first time the level of reproducibility that is achievable in high resolution stable isotope geochemistry of fossil tufa stromatolites. Three independent sample transects produce δ^{18}O and δ^{13}C data sets with identical means and highly similar ranges and standard deviations. Variations >0.5‰ in both δ^{18}O and δ^{13}C are non-random and attributable mainly to environmental drivers at the time of tufa formation.

2. Direct comparison of results from this French Eemian tufa stromatolite with those from a Greek deposit of similar age, illustrate that the temporal relationship between lamina microfacies boundaries and seasonal δ^{18}O reversals are critical information that may help distinguish between seasonality where temperature transitions are gradual (NW France) from those where changes are more abrupt due to e.g., summer aridity.

3. Overall the microfacies signal and likely range in seasonal temperatures inferred from the δ^{18}O values suggest our French Eemian tufa stromatolite formed in a climate with similar seasonality to the present day. We cannot yet be sure of absolute temperature differences between seasons but we are pursuing this issue with on-going clumped isotope geochemistry (see e.g. Eiler 2011).

References:

Andrews, J.E. and Brasier, A.T., 2005. Seasonal records of climatic change in annually laminated tufas: short review and future prospects. J Quaternary Sci, 20, 411-421.

Andrews, J.E., 2006. Paleoclimatic records from stable isotopes in riverine tufas : Synthesis and review. Earth-Sci Rev, 17, 85-104.

Andrews, J.E., Riding, R., and Dennis, P.F., 1997. The stable isotope record of environmental and climatic signals in modern terrestrial microbial carbonates from Europe, Palaeogeogr Palaeocl, 129, 171-189.

Antoine, P., Catt, J., Lautridou, J.P., and Sommé, J., 2003. The loess and coversands of Northern France and Southern England. J Quaternary Sci, 18, 309-318.

Antoine, P., Limondin Lozouet, N., Chaussé, C., Lautridou, J.-P., Pastre, J.-F, Auguste, P., Bahain, J.-J., Falguères C., and Ghaleb, B., 2007. Pleistocene fluvial terraces from northern France (Seine, Yonne, Somme): synthesis, and new results from interglacial deposits. Quaternary Sci Rev, 26, 2701-2723.

Antoine, P., Limondin-Lozouet, N., Auguste, P., Locht, J.L., Ghaleb, B., Reyss, J.L., Escudé, E., Carbonel, P., Mercier, N., Bahain, J.J., Falguères, C., and Voinchet, P., 2006. Le tuf de

Caours (Somme, France) : mise en évidence d'une séquence éemienne et d'un site paléolithique associé. Quaternaire, 17, 281-320.

Bahain, J.-J, Falgueres, C., Dolo, J.-M., Antoine, P, Auguste, P., Limondin-Lozouet, N., Locht, J.-L., and Tuffreau, A., 2010. ESR/U-series dating of teeth recovered from well-stratigraphically age-controlled sequences from Northern France. Quaternary Geochronology, 5, 371-375.

Bowen, G. J., and Revenaugh, J., 2003. Interpolating the isotopic composition of modern meteoric precipitation. Water Resources Research, 39, 1299-1312.

Brasier, A. T., Andrews, J. E., and Kendall, A. C., 2011. Diagenesis or dire genesis? The origin of columnar spar in tufa stromatolites of central Greece and the role of chironimid larvae. Sedimentology, 58, 1283-1302.

Brasier, A.T., Andrews, J.E., Marca-Bell, A.D., and Dennis, P.F., 2010. Depositional continuity of seasonally laminated tufas: Implications for δ^{18}O based palaeotemperatures. Global Planet Change, 71,160-167.

Chafetz, H.S. and Folk, R.L., 1984. Travertines: depositional morphology and the bacterially constructed constituents. J Sediment Petrol, 54, 289-316.

Clark, I.D. and Fritz, P., 1997. Environmental isotopes in hydrogeology. Lewis, Boca Raton

Coplen, T.B., 2007. Calibration of the calcite–water oxygen isotope geothermometer at Devils Hole, Nevada, a natural laboratory. Geochim Cosmochim Ac, 71, 3948-3957.

Craig, H., 1965. The measurement of oxygen isotope palaeotemperatures, In Tongiorgi, E. (ed.): Stable Isotopes in Oceanographic Studies and Palaeotemperatures. Consiglio Nazionale Delle Ricerche, Laboratorio di Geologia Nucleare, Pisa, 161-182.

Dabkowski, J., Limondin-Lozouet, N., Antoine, P., Marca-Bell, A., and Andrews J., 2011. Enregistrements des variations climatiques au cours des interglaciaires pléistocènes d'après l'étude des isotopes stables de la calcite des tufs calcaires. Quaternaire, 22 (4), 275-281.

Dabkowski, J., Antoine, P., Limondin-Lozouet, N., Chaussé, C., and Carbonel, P., 2010. Les microfaciès du tuf calcaire éemien (SIM 5e) de Caours (Somme, France) : éléments d'analyse paléoéocologique du dernier interglaciaire. Quaternaire, 21, 127-137.

Darling, W.G., 2004. Hydrological factors in the interpretation of stable isotopic proxy data present and past: a European perspective, Quaternary Sci Rev, 23, 743-770.

Dray, M., Ferhi, A., Jusserand, C., and Olive, P., 1998. Palaeoclimatic indicators deduced from isotopic data in the main French deep aquifers. Proceeding of a symposium IAEA, Vienna, 14-18 April 1997, Isotope Techniques in the Study of Environmental Change, 683-692.

Eiler, J.M., 2011. Palaeoclimate reconstruction using carbonate clumped isotope thermometry. Quaternary Science Reviews, 30, 3575-3588.

Freytet, P. and Plet, A., 1991. Les formations stromatolitiques (tufs calcaires) récentes de la région de Tournus (Saône-et-Loire), Geobios-Lyon, 24, 123-139.

Freytet, P. and Plet, A., 1996. Modern freshwater microbial carbonates: the *Phormidium* stromatolithes (tufa-travertine) of Southeastern Burgundy (Paris Basin, France), Facies, 34, 219-238.

Freytet, P. and Verrecchia, E., 1998. Freshwater organisms that build stromatolites: a synopsis of biocrystallization by prokariotic algae, Sedimentology, 45, 535-563.

19

Freytet, P., 1990. Contribution à l'étude des tufs calcaires (édifices stromatolithiques) du bassin de Paris. Les organismes constructeurs, aspects microscopiques, Bulletin du Centre de Géomorphologie de Caen, 38.

Freytet, P., 1992. Les cristallisations de calcite associées à des restes de végétaux (algues, feuilles) en milieu fluviatile et lacustre, actuel et ancien (tufs et travertins), B Soc Bot Fr, 139, 69-74.

Freytet, P., 1997. Non marine Permian to Holocene algae from France and adjacent country. Part 1. Ann Paleontol, 83,289-332.

Freytet, P., 1998. Non marine Permian to Holocene algae from France and adjacent country. Part 2. Ann Paleontol, 84, 3-51.

Garnett, E.R., Andrews, J.E., Preece, R.C., and Dennis, P.F., 2004. Climatic chance recorded by stable isotopes and trace elements in a British Holocene tufa, J Quaternary Sci, 19, 251-262.

Hays, P.D., and Grossman, E.L., 1991. Oxygen isotopes in meteoric calcite cements as indicators of continental palaeoclimate. Geology, 19, 441-444.

Hendy, C.H., 1971. The isotopic geochemistry of speleothems--I. The calculation of the effects of different modes of formation on the isotopic composition of speleothems and their applicability as palaeoclimatic indicators, Geochim Cosmochim Ac, 35, 801-824.

Hori, M., Kawai, T., Matsuoka, J., and Kano, A., 2009. Intra-annual perturbations of stable isotopes in tufas: Effects of hydrological processes, Geochim Cosmochim Ac, 73, 1684-1695.

IAEA/WMO: Global Network of Isotopes in Precipitation, 2006. The GNIP Database.
Accessible at: http://www.iaea.org/water

Ihlenfeld, C., Norman, M. D., Gagan, M. K., Drysdale, R. N., Maas, R., and Webb, J., 2003. Climatic significance of seasonal trace element and stable isotope variations in a modern freshwater tufa. Geochim Cosmochim Ac, **67**, 2341-2357.

Janssen, A., 2000. Petrography and geochemistry of active and fossil tufa deposits from Belgium. Katholieke Universiteit, Leuven.

Janssen, A., Swennen, R., Podoor, N., and Keppens, E., 1999. Biological and diagenetic influence in recent and fossil tufa deposits from Belgium, Sediment Geol, 126, 75-95.

Kano, A., Matsuoka, J., Kojo, T., and Fujii, H., 2003. Origin of annual laminations in tufa deposits, southwest Japan. Palaeogeography, Palaeoclimatology, Palaeoecology, 191 (2), 243-262.

Kano, A., Hagiwara, R., Kawai, T., Hori, M., and Matsuoka, J., 2007. Climatic conditions and hydrological change recorded in a high-resolution stable isotope profile of a recent laminated tufa on a subtropical island, southern Japan. J. Sediment. Res. 77, 59–67.

Kawai, T., Kano, A. and Hori, M., 2009. Geochemical and hydrological controls on biannual lamination of tufa deposits,*Sedimentary Geology*, 213, 41-50,

Kim, S.T. and O'Neil, J.R., 1997. Equilibrium and nonequilibrium oxygen isotope effects in synthetic carbonates. Geochim Cosmochim Ac, 61, 3461-3475.

Leng, M.J., Lamb, A.L., Heaton, T.H., Marshall, J.D., Wolfe, B.B., Jones, M.D., Holmes, J.A., and Arrowsmith, C., 2006. 4. Isotope in lake sediments, In M. Leng, (ed.) Isotopes in Palaeoenvironmental Research. Springer, Netherlands, 10, 147-184.

Liu, Z., Sun, H., Lu, B., Liu, X., Ye, W. and Zeng, C., 2010. Wet-dry seasonal variations of hydrochemistry and carbonate deposition rates in a travertine-depositing canal at Baishuitai,

Yunnan, SW China: Implications for the formation of biannual laminae in travertine and for climatic reconstruction. Chemical Geology, 273, 258-266.

Matsuoka, J., Kano, A., Oba, T., Wanatabe, T., Sakai, S., and Steto, K., 2001. Seasonal variation of stable isotopic compositions recorded in a laminated tufa, SW Japan, Earth Planet Sc Lett, 192, 31-44.

McManus, J.F., Bond, G., Broecker, W.S., Johnsen, S., Labeyrie, L., and Higgins, S., 1994. High-resolution climate records from the North Atlantic sduring the last interglacial. Nature, 371, 326-329.

Mickler, P.J.B., Jay L., Stern, L., Asmeron, Y., Edwards, L., and Ito, E., 2004. Stable isotope variations in a modern tropical speleothems: Evaluating equilibrium vs. kinetic isotope effects. Geochim Cosmochim Ac, 68, 4381-4393.

Mischke, S., and Zhang, C., 2008. A laminated tufa carbonate from the mid Holocene of the Qilian Mountains and its potential for palaeoclimate inferences. Episodes, 31, 401-407.

Monty, C., 1976. The origin and development of cryptalgal fabrics. In: Walter, M. (ed.) *Stromatolites: Developments in Sedimentology 20*. Amsterdam: Elsevier, 193-249.

O'Brien, G.R., Kaufman, D.S., Sharp, W.D., Atudorei, V., Parnell, R.A., and Crossey, L.J., 2006. Oxygen isotope composition of annually banded modern and mid-Holocene travertine and evidence of paleomonsoon floods, Grand Canyon, Arizona, USA, Quaternary Res, 65, 366-379.

Pedley, HM, 1990. Classification and environmental models of cool freshwater tufas. Sedimentary Geology, 68, 143–154.

Sánchez-Goñi, M.F, 2007. Introduction to climate and vegetation in Europe during MIS 5, In F. Sirocko et al., (eds.), The climate of the past Interglacials. Elsevier, Amsterdam, 197-205.

Sun, H., Liu, Z. and Yan, H., 2014. Oxygen isotope fractionation in travertine-depositing pools at Baishuitai, Yunnan, SW China: effects of deposition rates. Geochim Cosmochim Ac, 133, 340–350.

Van Kolfschoten, T., Gibbard P., and Knudsen, K.-L., 2003. The Eemian interglacial: a Global Perspective. Introduction, Global Planet Change, 36, 147-149.

Watkins, J.M., Nielsen, L.C., Ryerson, F.J. and DePaolo, D.J., 2013. The influence of kinetics on the oxygen isotope composition of calcium carbonate. Earth and Planetary Science Letters, 375, 349-360.

Figure 1. A. Location map of the Caours tufa ; B. East profile of the S2 excavation Sector in 2005 (Antoine et al., 2006; modified); C. detail of the tubular facies at top of a localised channel.

Figure 2. Cross section of the Caours tubular stromatolite sampled for high-resolution analyses and photomicrographs of fabrics observed in thin section. Microfacies in red boxes are interpreted as "summer" laminae, including the two continuous sparitic layers interrupting Microfacies IV (red arrows); microfacies in blue boxes grew under cooler conditions (see text for detailed description and interpretation). Str-HRr, Str-HRc, Str-HR and Str-HR 2 show positions of sampled transects.

Figure 3. High-resolution stable isotope data transects (δ^{18}O and δ^{13}C) in the Caours stromatolite versus distance (in mm) from the most central sample. The distribution of data within the laminar microfacies can be seen from the microfaies column on the left (from Fig. 2). The red colour of Microfacies I indicates "summer" conditions, alternating with blue coloured microfacies (II-IV) that formed under cooler conditions according to microfacies interpretation (see text for details). Blue and red boxes on the isotope profiles represent partial mean values for each lamina relative to the median value for the whole transect. Lower values are generally recorded in "summer" facies (red notation) whereas higher values are observed in "winter" facies (blue notation). A 4-point running mean for each transect (same symbols, dots for Str-HRr etc.) is shown on the right.

Figure 4. Microfacies and high resolution calcite δ^{18}O data transect from MIS 5 Zemeno laminated tufa (Central Greece; Brasier at al., 2010) compared to the Caours data (this study: running mean values; see Fig. 3 for key to symbols). The data are shown on a common depth

24

scale. At Zemeno the α bands represent summer laminae and the β bands winter; at Caours red layers are 'summer' and blue layers are 'cooler' (Fig. 2). Horizontal lines tie petrography with stable isotopes and arrows show the main reversals in both sections: reversals are abrupt and correlated to laminae boundaries at Zenemo while they occur within laminae at Caours.

B S2-2005 East Profile
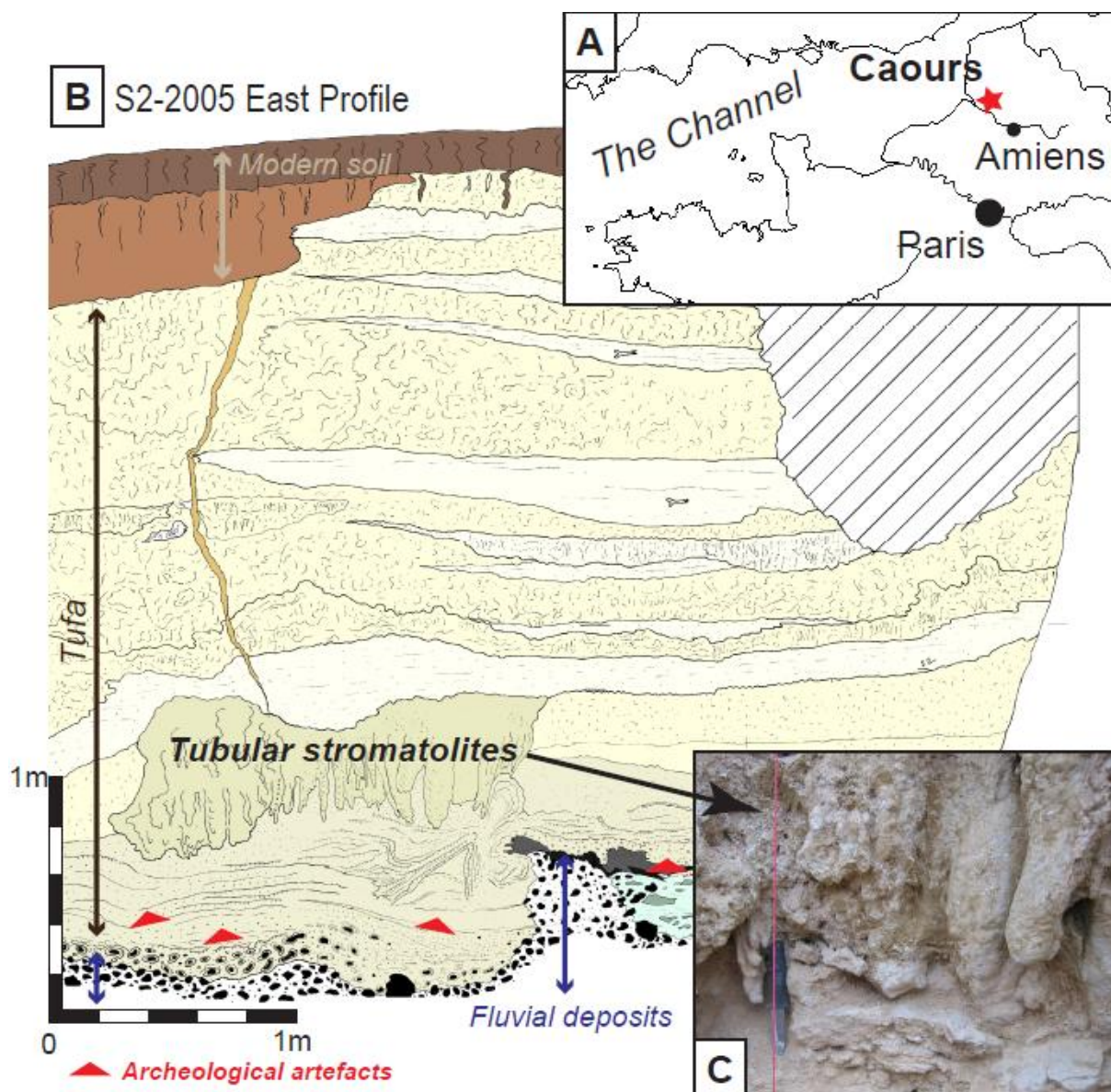
Modern soil

Tufa

Tubular stromatolites

1m

0   1m

▲ *Archeological artefacts*

Fluvial deposits

A

The Channel

Caours

Amiens

Paris

C

Fig. 1

Microfacies I: Elongate calcite spar crystals including imprints of cyanobacterial fascicules

Microfacies II: Microsparitic and micritic laminae with interne lamination

Microfacies III: Disorganised laminae of sparitic crystals

Microfacies IV: Clotted micritic lamina without structure

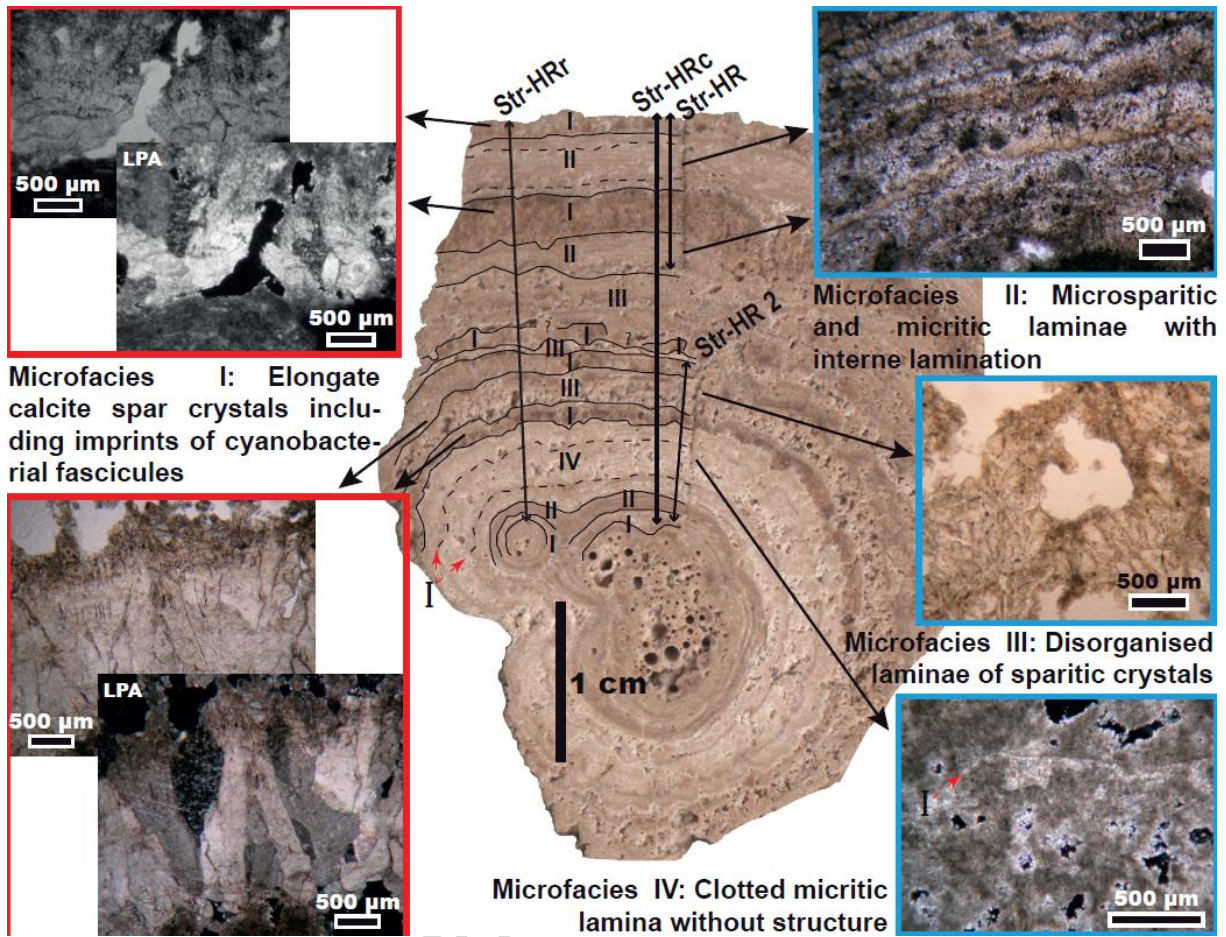Fig. 2

27
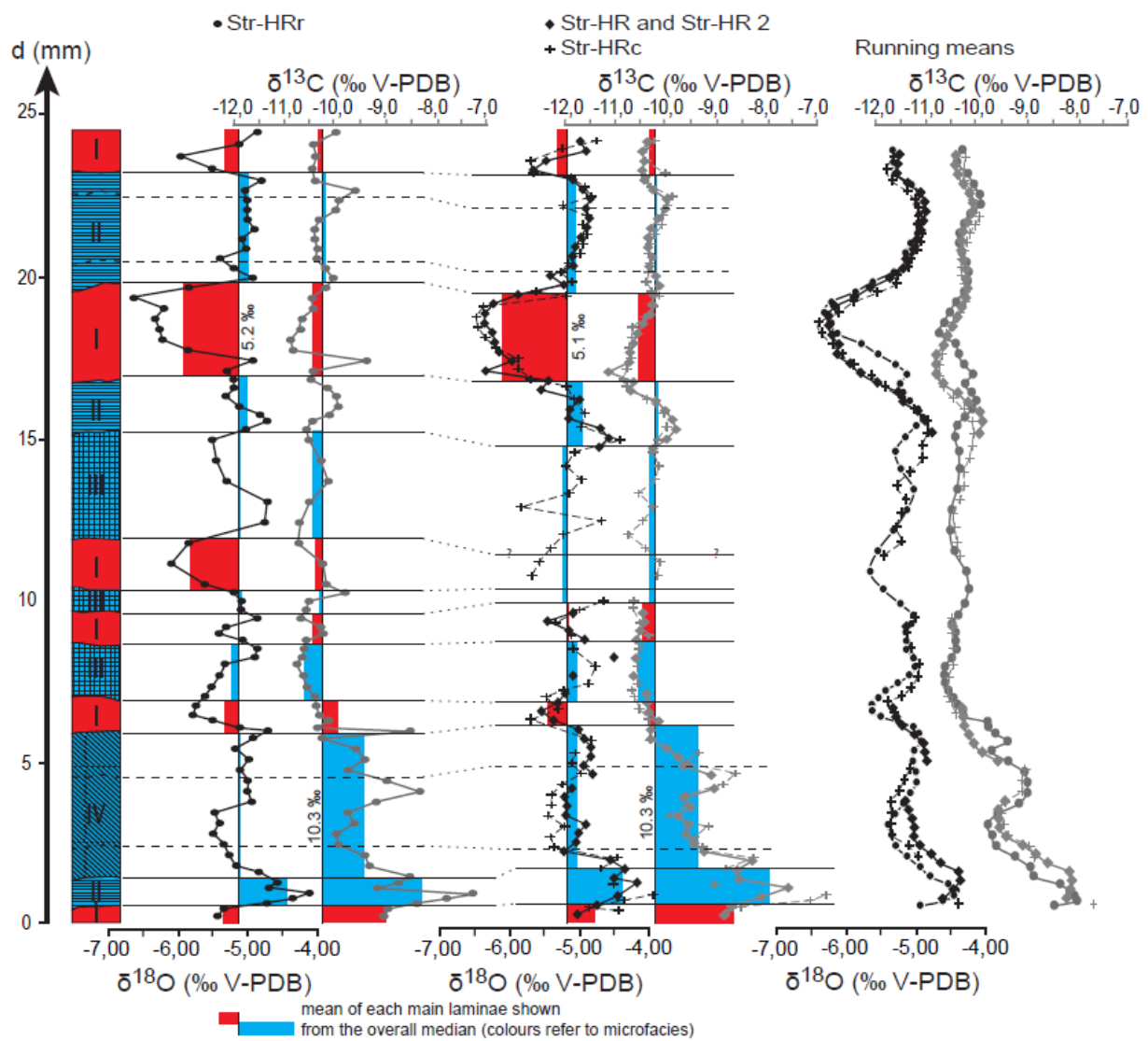
Fig. 3

Fig. 4

Table 1

	Str-HR and Str-HR 2 (initial transect) n= 63		Str-HRc (continuous) n= 70		Str-HRr (replicate) n= 78	
	$\delta^{18}O$	$\delta^{13}C$	$\delta^{18}O$	$\delta^{13}C$	$\delta^{18}O$	$\delta^{13}C$
Minimum	-6.4	-11.2	-6.5	-10.8	-6.6	-10.9
Maximum	-4.2	-7.5	-3.9	-6.8	-4.1	-7.3
Mean value	-5.2	-10.0	-5.2	-10.0	-5.2	-10.0
Standard deviation	0.5	0.7	0.5	0.8	0.5	0.7
Precision			< 0.1 for all			
$\delta^{18}O$-$\delta^{13}C$ correlation (r^2)	0.35		0.27		0.26	

Table 2

Month	1	2	3	4	5	6	7	8	9	10	11	12
	63	49	57	53	59	66	59	70	65	82	80	80

Table 3

Month	1	2	3	4	5	6	7	8	9	10	11	12
Brest-Plouzane (48°21'N; 4°34'W)	-5,23	-4,91	-4,78	-5,38	-5,89	-3,94	-3,24	-4,04	-4,66	-4,74	-5,55	-5,74
Liège (50°42'N; 5°28'E)	-8,34	-9,38	-7,06	-6,02	-5,82	-4,91	-4,36	-5,59	-5,72	-7,27	-9,15	-8,28
Orléans La Source (47°54'N; 1°54'E)	-7,81	-6,52	-5,46	-6,02	-5,51	-4,78	-4,96	-5,33	-5,56	-6,89	-7,6	-7,56

Table 4

| Equation | Range of estimated temperatures (°C) | | ΔT |
	Maximum (from calcite $\delta^{18}O$ = -6.3‰)	Minimum (from calcite $\delta^{18}O$ = -4.2‰)	
Case 1: $\delta^{18}O_{water}$ = -7‰ (Value for Holocene groundwater, Paris Basin; Dray et al. 1998)			
Craig (1965)	**12.9**	**5.5**	7.7
Hays and Grossman (1991)	**12.7**	4.4	8.3
Kim and O'Neil (1997)	**11.6**	2.4	9.2
Coplen (2007)	**18.3**	**8.4**	9.9
Case 2: $\delta^{18}O_{water}$ = -6.7‰ (Value for modern Caours summer recharge – Apr-Oct, OIPC)			
Craig (1965)	**14.2**	**6.2**	8.0
Hays and Grossman (1991)	**14.0**	**5.6**	8.4
Kim and O'Neil (1997)	**13.0**	3.7	9.3
Coplen (2007)	**19.8**	**9.7**	10.1
Case 3: $\delta^{18}O_{water}$ = -9‰ (Value for modern Caours winter recharge – Nov-March, OIPC)			
Craig (1965)	5.5	-1.2	6.6
Hays and Grossman (1991)	4.8	-2.5	7.3
Kim and O'Neil (1997)	2.8	-5.8	8.6
Coplen (2007)	8.8	-0.5	9.3

Table 1. High resolution stable isotope data (in ‰ V-PDB) transect summaries.Table 2. Monthly modern precipitation amount at Abbeville (in mm; from 1981 to present MétéoFrance surveys).

Table 2. Monthly modern precipitation amount at Abbeville (in mm; from 1981 to present MétéoFrance surveys).

Table 3. Data summaries of present day δ^{18}O composition of rainfall at the nearest GNIP site to Caours (in ‰ V-SMOW; Global Network of Isotopes in Precipitations; IAEA/WMO, 2006). The maximum and minimum δ^{18}O values are bold and correspond respectively to summer and winter conditions.

Table 4. Range of maximum/minimum palaeotemperature solutions estimated from calcite δ^{18}O minimal and maximum values for Caours stromatolithe and $\delta^{18}O_{water}$ values representing a range of likely water isotopic compositions (see text for details). The four palaeotemperature equations represent a range of commonly used equilibrium formulations: Kim and O'Neil (1997) is used widely today, although Sun et al. (2014) found it most appropriate for fast depositing tufas; slower growing tufa calcites were better described by the Coplen (2007) relationship. Results in bold represent values in the range 5-20 ˚C, which is considered an acceptable likely window of temperatures based on modern stream water temperatures (see text).

Highlights:

► Eemian climate of NW France was seasonal with similar temperature range to present;

►Combining petrography with high resolution δ^{18}O data identifies style of seasonality;

►First assessment of high resolution δ^{18}O reproducibility in fossil laminated tufa.